

## CHARACTERIZATION OF THROUGH-WALL AEROSOL TRANSMISSION FOR SCC-LIKE GEOMETRIES

Samuel G. Durbin, Eric R. Lindgren, and Ramon J.M. Pulido

*Sandia National Laboratories, P.O. Box 5800, Albuquerque, NM 87123-1369 USA, sdurbin@sandia.gov*

*The flow rates and aerosol transmission properties were evaluated for an engineered microchannel with characteristic dimensions similar to those of stress corrosion cracks (SCCs) capable of forming in dry cask storage systems (DCSS) for spent nuclear fuel. Pressure differentials covering the upper limit of commercially available DCSS were also examined. These preliminary data sets are intended to demonstrate a new capability to characterize SCCs under well-controlled boundary conditions.*

### I. INTRODUCTION

Dry cask storage systems (DCSS) for spent nuclear fuel (SNF) are designed to provide a confinement barrier that prevents the release of radioactive material, maintain SNF in an inert environment, provide radiation shielding, and maintain subcritical conditions. SNF is initially stored in pools of water to provide cooling and radiation shielding. As these pools near capacity, dry storage systems are sought as the primary alternative for interim storage. After sufficient cooling in pools, SNF is loaded into a canister which is then welded shut. The dry storage canister is decontaminated, dried, and ultimately sent to a storage location for emplacement in an overpack.

Canisters are typically made of stainless steel. The open volume between the canister and the overpack allows for passive ventilation from outside air, which can impart dust that collects on the surfaces of the canister. As the SNF cools, salts contained in the dust may deliquesce to form concentrated brines. These brines may contain corrosive species such as chlorides that can lead to localized corrosion or “pitting”. With sufficient stresses, these pits can evolve into stress corrosion cracks (SCCs), which could penetrate through the canister wall and create a flow path from the interior of the canister to the external environment.<sup>1</sup>

#### I.A. Objective

The purpose of this study was to explore the flow rates and aerosol transmission through an engineered slot with characteristic dimensions similar to those in SCCs.

Additionally, pressure differentials covering the upper limit of commercially available DCSS were studied. Given the scope and resources available, these data sets are considered preliminary and are intended to demonstrate a new capability to characterize SCC under well-controlled boundary conditions. Additional information on this exploratory study is available in the project report.<sup>2</sup>

#### I.B. Previous Studies

Data obtained from the measurement of particulate segregation in flows through open channels has significance in multiple fields. Studies include particle penetration through building cracks,<sup>3, 4, 5</sup> nuclear reactor safety,<sup>6</sup> and more recently, storage and transportation of spent nuclear fuel in dry casks. Study of these systems contribute to the understanding of particulate segregation through small channels as functions of particle size, channel dimensions, and differential pressures.

Previous work has contributed to the characterization of particulate segregation across channel flow for a range of particle sizes in aerosols. Lewis was motivated by a lack of empirical studies to support the development of protection factors against solid particles for enclosures.<sup>3</sup> This protection factor was taken as the ratio of the dose of an outside concentration of particulates to the dose accumulated inside an enclosure for a specified time, with the doses defined as concentration-time integrals. Models were derived describing the total transport fraction of particles across a rectangular slot into an enclosure as functions of particle size, differential pressures, and slot heights. Lewis described an experimental apparatus with synthesized aerosols (containing either talc, aluminum oxide, titanium oxide, various silica powders, or ambient dust) mixed in a chamber containing an enclosure with a rectangular slot open to the chamber.<sup>3</sup> A differential pressure was established between the chamber and the enclosure. Protection factors were found by comparing mass concentration values inside and outside the enclosure over a given time. The primary observations included the decrease in total transport fraction with increasing particle size from 1-10  $\mu\text{m}$  as well as a decrease in protection factor

(corresponding to an increase in total transport fraction) with increasing differential pressures and slot heights.

Liu and Nazaroff conducted experiments of aerosol flow through rectangular slots using various building materials, including aluminum, brick, concrete, and wood.<sup>4</sup> The slot heights were 0.25 mm and 1 mm, which are quite large compared to the micron- to submicron-sized particles they flowed through the cracks. They obtained data for particle penetration (defined as the ratio of downstream to upstream particle concentration), related to total transport fraction, as a function of particle size and found that, for 0.25 mm cracks, particle sizes between 0.1-1  $\mu\text{m}$  achieved penetration factors near unity, while smaller and larger particles showed diminished penetration factors for pressure differentials of 4 and 10 Pa. Meanwhile, for 1 mm slot heights, the penetration factors were near unity across most of the particle size distribution. Liu and Nazaroff's results matched closely with models they created from analysis of particle penetration through simplified cracks and had similar qualitative conclusions to Lewis's work.<sup>7</sup>

Mosley *et al.* studied particle penetration through a 0.508 mm slot height using aluminum; the particle size distribution was 0.5-5  $\mu\text{m}$  (Ref. 5). They found penetration factors close to unity for particle sizes between 0.1-1  $\mu\text{m}$ , with a sharp drop-off in penetration factor for particle sizes larger than 1  $\mu\text{m}$  for pressure differentials between 2 and 20 Pa. This observation was consistent with Liu and Nazaroff's results when considering the order of magnitude of the pressure differentials and particle size distributions.

### I.C. Uniqueness of Current Study

The motivation behind the aforementioned work was based on ambient particle penetration of enclosures and the amount of particles subject to human exposure, with slot heights and pressure differentials corresponding to conditions typically associated with building cracks and pressure differences between indoor and outdoor environments, respectively. However, the channel dimensions considered do not apply to the channel geometry associated with SCC from potential corrosion of dry casks. The literature reports typical crack heights to be around 16 to 30  $\mu\text{m}$  (Refs. 8, 9, and 10) and internal pressures of 100 to 760 kPa (14.5 to 110 psig) (Ref. 9) for a range of cask models. Therefore, an apparatus and procedures were developed to investigate a slot height on the order of tens of microns and pressure differentials on the order of hundreds of kPa to supplement the established database of particulate transmission in microchannel flows. This experimental approach is intended to be adaptable for future testing of more prototypic stress corrosion crack geometries.

## II. APPARATUS AND PROCEDURES

The experimental approach adopted for this study is similar to previous studies in that aerosol analyzers are used to characterize the particle size distribution and concentration present in the gas before and after flowing through a simulated crack.<sup>3, 4, 5, 7</sup> As these previous studies considered aerosol transport through building walls or containment structures, the focus was placed on flows through relatively wide and long slots driven by constant low pressure drops. In the present study, consideration is given to aerosol transport through dry storage canister walls. Here, the focus is on much narrower and shorter microchannels that represent stress corrosion cracks through the canister wall driven by initially higher pressure drops. Furthermore, the pressure drop is not constant but transient to simulate the blowdown from canister depressurization.

### II.A. General Construction

The general layout of the experimental setup is illustrated in Figure 1. A 0.908 m<sup>3</sup> (240 gal) pressure tank is used to simulate the canister. The tank was pressurized and loaded with a measured amount of aerosols. Flow from the tank into the test section was measured by a mass flow meter (MFM). The engineered microchannel, simulating a crack, was mounted in the middle of the test section. A sample stream was metered from the high-pressure upstream and low-pressure downstream side of the simulated crack for aerosol size and concentration characterization using identical TSI Model 3321 Aerodynamic Particle Sizer (APS) Spectrometers. The pressure of the upstream sample was reduced to ambient by a mass flow controller (MFC) that metered the flow to the upstream APS. An open-to-ambient, overflow line was used to protect the upstream APS from over-pressurization in the event of a control valve failure. A mass flow meter measured the sample flow drawn into the downstream APS. Pressure was monitored on the upstream and downstream sides of the microchannel using pressure transducers (PTs). A low pressure drop high efficiency particulate air (HEPA) filter was used to remove aerosols from the exhaust stream.

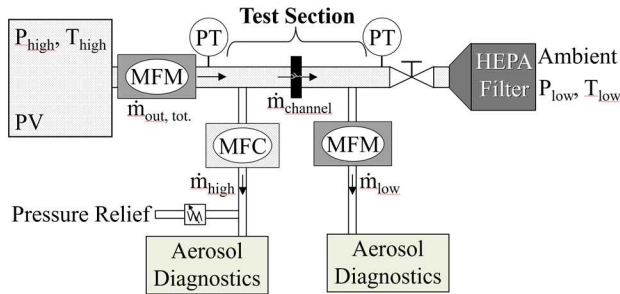


Fig. 1. Schematic of the apparatus showing the major components.

## II.B. Design of the Microchannel

The engineered microchannel was fabricated from paired high-precision Mitutoyo gage blocks. The microchannel was machined into the surface of one gage block using electrical discharge machining (EDM). The mounting holes were also cut using wire EDM. As shown in Figure 2 the dimensions of the microchannel are 12.7 mm (0.500 in.) wide, 8.86 mm (0.349 in.) long and an average of 28.9  $\mu\text{m}$  (0.0011 in.) deep. The paired halves of the gage blocks are bolted together to form the microchannel held in a mounting assembly. An isometric view of the microchannel mounted to the flow flange is shown in Figure 3.

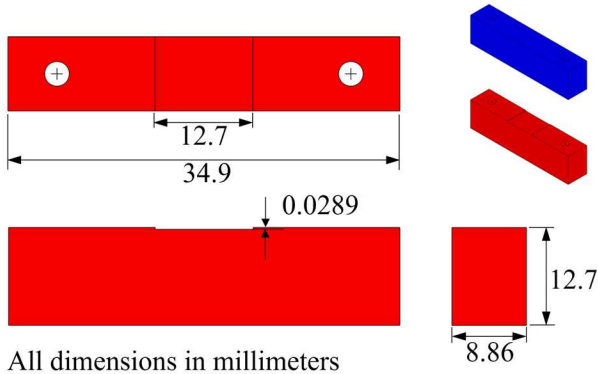


Fig. 2. Schematic of the microchannel assembly.

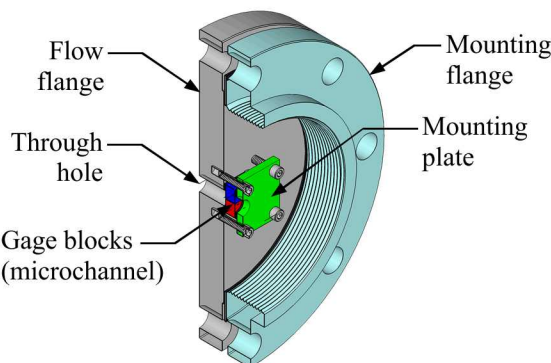


Fig. 3. Isometric cutaway showing the microchannel mounted to the flow flange.

## II.C. Selection of Initial Conditions

### II.C.1. Surrogate Selection

Cerium oxide ( $\text{CeO}_2$ ) was chosen as the surrogate for spent nuclear fuel ( $\rho_{\text{SNF}} \approx 10 \text{ g/cm}^3$ ) because of its relatively high density ( $\rho_{\text{CeO}_2} = 7.22 \text{ g/cm}^3$ ) and its commercial availability. All values are defined here as aerodynamic equivalent diameter (AED). This surrogate was chosen because the particles were concentrated in the respirable range ( $\text{AED} < 10 \mu\text{m}$ ). Table 1 gives a summary of the aerosol size distribution statistics of the surrogate as measured by the same TSI 3321 instrument in a separate characterization study.

Table 1. Summary of cerium oxide surrogate characteristics.

	Number Particle Size	Mass Particle Size
Median ( $\mu\text{m}$ )	1.18	4.12
Mean ( $\mu\text{m}$ )	1.36	4.81
Geometric Mean ( $\mu\text{m}$ )	1.24	3.98
Mode ( $\mu\text{m}$ )	1.07	4.22
Geometric Std. Dev.	1.47	1.88
Total Concentration	2422 (#/ $\text{cm}^3$ )	2.30 (mg/ $\text{m}^3$ )

### II.C.2. Selection of Aerosol Density

An upper estimate of the desired aerosol density was needed to inform the execution of the tests. As described earlier, the tests described in this report were focused on respirable particles with an  $\text{AED} < 10 \mu\text{m}$ . To derive an aerosol density of interest, data from a previous study was referenced to estimate an upper bound for release of spent fuel into a canister.<sup>11</sup> An average release fraction across all tests was found to be  $1.9 \times 10^{-5}$ , where air was blown through segments of spent fuel rods and the released fuel was measured. Of this release fraction, the respirable fraction from all available data was  $6.0 \times 10^{-3}$ . Therefore, the respirable release fraction was estimated as the product of the two fractions as  $1.1 \times 10^{-7}$ .

To estimate an upper aerosol density for spent fuel dry storage, a canister with 37 pressurized water reactor (PWR) assemblies with a mass of fuel ( $\text{UO}_2$ ) 520 kg per assembly was assumed. Ten percent of the fuel was assumed to fail due to an undefined event. The fines released were assumed to recirculate within the canister without any deposition. The canister was assumed to have a starting initial pressure of 800 kPa (116 psia). The equivalent aerosol density for this assumed system at standard

temperature and pressure is approximately  $7 \text{ mg/m}^3$ . For the storage tank, approximately 50 mg was needed to achieve an equivalent aerosol density. Expecting a large deposition factor, the test was started with an excess ( $\sim 100 \text{ mg}$ ) of the respirable ceria particles aerosolized into the tank.

### III. PRELIMINARY RESULTS

#### III.A. Gas Flow Measurements

Figure 4 shows the mass flow of air through the microchannel as a function of pressure drop across the microchannel. A pre-test characterization (blue) with zero particle loading was collected using clean air and a clean microchannel. The data collected during the aerosol-laden test is shown in red. The post-test characterization (green) was conducted with zero particle loading and clean air but with the previously deposited aerosols on the microchannel left in an undisturbed state. Figure 5 shows a photo of the gage blocks making up the microchannel after the aerosol-loaded test and the post-test characterization. The microchannel is cut into the gage block in the foreground and particle deposition is evident, especially along the side walls of the microchannel. The decrease in flow rate from the pre-test characterization test to the aerosol test indicates partial plugging of the microchannel. The similarity of the aerosol test results and the post-test characterization results indicates that the microchannel particle deposition occurred early in the aerosol test.

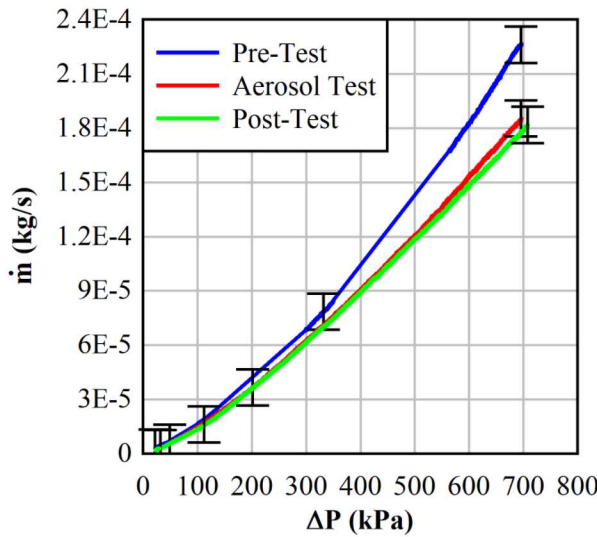


Fig. 4. Mass flow rate versus pressure differential.

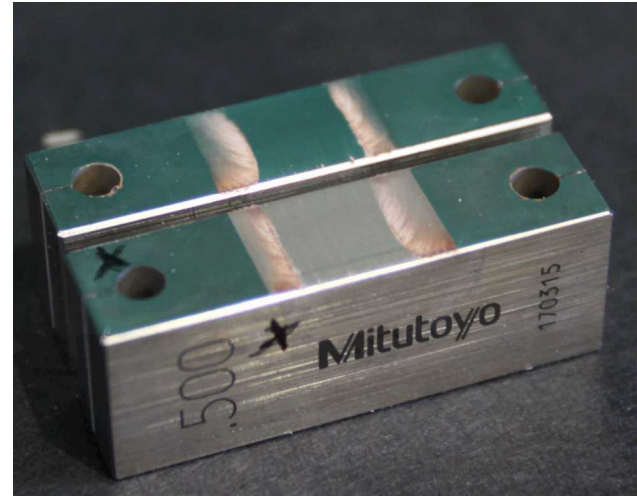


Fig. 5. Photo of gage block microchannel. The microchannel is cut into the block in the foreground. Particle deposition is evident along the side walls of the microchannel.

#### III.B. Aerosol Measurements

Figure 6 shows the mass concentration of aerosols measured upstream and downstream of the microchannel on the left independent axis and the air mass flow rate through the microchannel on the right independent axis as a function of time. The mass concentration of aerosols is higher upstream of the microchannel than downstream indicating exclusion of aerosols in the flow through the microchannel. The concentration difference is greatest early in the transient when the flow through the microchannel is largest. Later, the concentrations become equivalent after approximately five hours. Over the nine-hour period, the average mass concentration upstream was  $0.048 \text{ mg/m}^3$  while the average concentration downstream was  $0.030 \text{ mg/m}^3$ . The transient aerosol mass flow rate and integral total aerosol mass is shown in Figure 7. By the end of the test, the mass of aerosols that entered the test section upstream of the microchannel was 0.207 mg and the mass of aerosols that exited the microchannel was 0.117 mg.

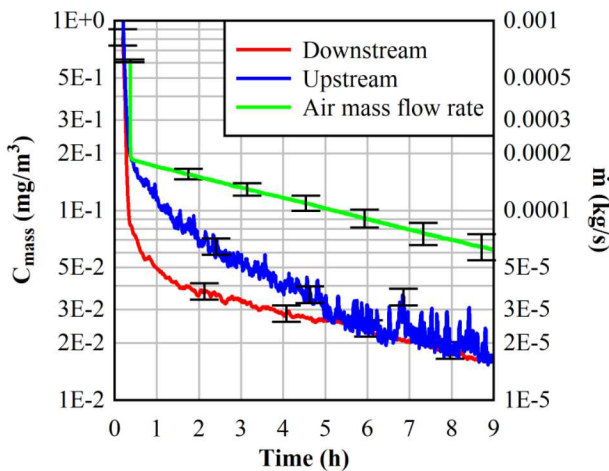


Fig. 6. Air mass flow rate through the microchannel and the aerosol mass concentration for upstream and downstream sampling as a function of time.

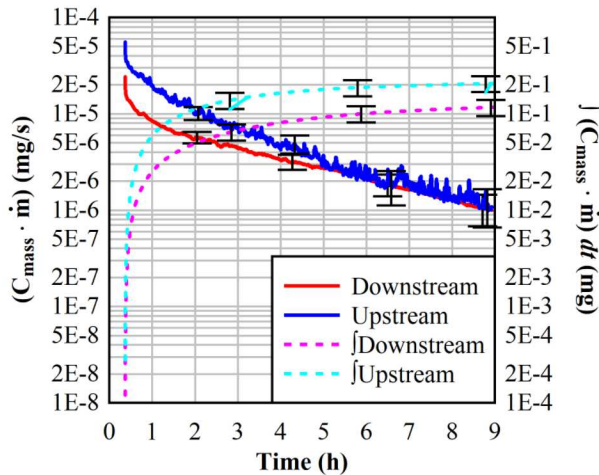


Figure 7. Transient aerosol mass flow rate and integral total aerosol mass.

#### IV. SUMMARY

The gap of the microchannel tested was 28.9  $\mu\text{m}$  (0.0011 in.), the width was 12.7 mm (0.500 in.) and the length was 8.86 mm (0.349 in.). Over a nine-hour period, the average mass concentration upstream of the microchannel was 0.048  $\text{mg}/\text{m}^3$  while the average concentration downstream was 0.030  $\text{mg}/\text{m}^3$ . At the end of the test, the integrated mass of aerosols entering the test section upstream of the microchannel was 0.207 mg and the mass of aerosols exiting the microchannel was 0.117 mg for an overall transmission of 0.56.

#### V. FUTURE WORK

These studies were exploratory in nature and made use of existing aerosol characterization equipment that was

limited to sampling at atmospheric pressure. Although the test apparatus was adapted to accommodate this constraint, the accuracy and uncertainty of future results are expected to improve by employing a high-pressure aerosol instrument in future testing.

While providing a well-controlled flow path for modeling and scoping studies, a slot orifice is a gross simplification of a prototypic stress corrosion crack. More complicated flow geometries, including lab-grown SCC, are being considered for future studies.

#### ACKNOWLEDGMENTS

This work was funded by the U.S. Department of Energy, Office of Nuclear Energy Spent Fuel and Waste Disposition Research and Development Program.

The authors would like to express their appreciation to Andres Sanchez and Gabriel Lucero of Department 6633 (WMD Threats and Aerosol Science) for their critical assistance in performing these tests. Parallel modeling efforts by Stylianos Chatzidakis at Oak Ridge National Laboratory and Andrew Casella at Pacific Northwest National Laboratory of these tests is eagerly anticipated.

#### REFERENCES

1. Schindelholz, E., C. Bryan, and C. Alexander, "FY17 Status Report: Research on Stress Corrosion Cracking of SNF Interim Storage Canisters," SAND2017-10338R, Sandia National Laboratories, Albuquerque, NM, August (2017).
2. Durbin, S.G., E.R. Lindgren, and R.J.M. Pulido, "Measurement of Particulate Retention in Microchannel Flows," SAND2018-10522 R, Sandia National Laboratories, Albuquerque, NM, September (2018).
3. Lewis, S., "Solid Particle Penetration into Enclosures", *J. Hazardous Materials*, **43**, 195-216, (1995).
4. Liu, D-L. and W.W. Nazaroff, "Particle Penetration Through Building Cracks," *Aerosol Science and Technology*, **37**, 565-573, (2003).
5. Moseley, R.B., D.J. Greenwell, L.E. Sparks, Z. Guo, W.G. Tucker, R. Fortmann, C. Whitfield, "Penetration of Ambient Fine Particles into the Indoor Environment," *Aerosol Science and Technology*, **34**, 127-136, (2001).
6. Powers, D.A., "Aerosol Penetration of Leak Pathways – An Examination of the Available Data and Models," SAND2009-1701, Sandia National Laboratories, Albuquerque, NM, April (2009).
7. Liu, D-L. and W.W. Nazaroff, "Modeling Pollutant Penetration Across Building Envelopes," *Atmos. Environm.*, **35**, 4451-4462, (2001).
8. EPRI, "Flaw Growth and Flaw Tolerance Assessment for Dry Cask Storage Canisters," EPRI 3002002785

Electric Power Research Institute, Palo Alto, CA, October (2014).

- 9. EPRI, "Dry Cask Storage Welded Stainless Steel Canister Breach Consequence Analysis Scoping Study," EPRI 3002008192, Electric Power Research Institute, Palo Alto, CA, November (2017).
- 10. Meyer, R. M., *et al.*, "Evaluating Conventional NDE Methods for Crack Detection in Metal Canisters," Presentation at *Extended Storage Collaboration Program (ESCP)*, December 4, (2013).
- 11. Hanson, B.D., R.C. Daniel, A.M. Casella, R.S. Wittman, W. Wu (BSC), P.J. MacFarlan, and R.W. Shimskey, "Fuel-In-Air FY07 Summary Report," PNNL-17275, Pacific Northwest National Laboratory, Richland, Washington, September (2008).